Cellular/Molecular

Light-Evoked Lateral GABAergic Inhibition at Single Bipolar Cell Synaptic Terminals Is Driven by Distinct Retinal Microcircuits

Jozsef Vigh,[1] Evan Vickers,[2] and Henrique von Gersdorff [2]

[1]Department of Biomedical Sciences, Colorado State University, Ft. Collins, Colorado 80523, and [2]The Vollum Institute, Oregon Health & Science University, Portland, Oregon 97239

Inhibitory amacrine cells (ACs) filter visual signals crossing the retina by modulating the excitatory, glutamatergic output of bipolar cells (BCs) on multiple temporal and spatial scales. Reciprocal feedback from ACs provides focal inhibition that is temporally locked to the activity of presynaptic BC activity, whereas lateral feedback originates from ACs excited by distant BCs. These distinct feedback mechanisms permit temporal and spatial computation at BC terminals. Here, we used a unique preparation to study light-evoked IPSCs recorded from axotomized terminals of ON-type mixed rod/cone BCs (Mb) in goldfish retinal slices. In this preparation, light-evoked IPSCs could only reach axotomized BC terminals via the lateral feedback pathway, allowing us to study lateral feedback in the absence of overlapping reciprocal feedback components. We found that light evokes ON and OFF lateral IPSCs (L-IPSCs) in Mb terminals having different temporal patterns and conveyed via distinct retinal pathways. The relative contribution of rods versus cones to ON and OFF L-IPSCs was light intensity dependent. ACs presynaptic to Mb BC terminals received inputs via AMPA/KA- and NMDA-type receptors in both the ON and OFF pathways, and used TTX-sensitive sodium channels to boost signal transfer along their processes. ON and OFF L-IPSCs, like reciprocal feedback IPSCs, were mediated by both $GABA_A$ and $GABA_C$ receptors. However, our results suggest that lateral and reciprocal feedback do not cross-depress each other, and are therefore mediated by distinct populations of ACs. These findings demonstrate that retinal inhibitory circuits are highly specialized to modulate BC output at different light intensities.

Introduction

Visual signals in the retina must pass through bipolar cells (BCs) on their way to the brain, because BCs form the sole direct excitatory connection between photoreceptors and ganglion cells (GCs), whose axons form the optic nerve. In the inner plexiform layer (IPL), BCs also excite amacrine cells (ACs) and receive inhibitory input from ACs. This input may be either reciprocal inhibition, originating from ACs directly excited by a given BC, or lateral feedback inhibition, originating from ACs excited by other BCs. Elegant immunocytochemical studies in the rabbit retina elucidated the complexity of this synapse; each rod bipolar terminal is contacted by varicosities from ~25 different S1-type ACs and 50 different S2-type ACs (Zhang et al., 2002). In the goldfish retina, a single mixed rod/cone BC (Mb) axon terminal receives ~350 inhibitory AC synapses in the IPL (Witkovsky and Dowling, 1969), of which 50% are reciprocal and 50% are lateral synapses (Marc and Liu, 2000). This suggests that a tremendous amount of synaptic computation takes place at bipolar cell terminals to determine the amount of glutamate that is released onto GCs.

Reciprocal feedback is thought to make the output of BCs more transient (Euler and Masland, 2000), tuning it to the dynamic range of GCs (Vigh and von Gersdorff, 2005) and preventing the rapid depletion of presynaptic vesicle pools (Singer and Diamond, 2006). Reciprocal feedback has also been shown to undergo use-dependent plasticity (Vigh et al., 2005; Li et al., 2007). Lateral feedback allows for spatial integration of signals (Cook and McReynolds, 1998), mediates center-surround organization of the receptive fields (Jacobs and Werblin, 1998; Ichinose and Lukasiewicz, 2005; Zhang and Wu, 2009), and contributes to GC orientation selectivity (Venkataramani and Taylor, 2010).

It is difficult to distinguish these forms of feedback when the retina is stimulated with its natural stimulus, light, because some ACs might provide both lateral and reciprocal feedback to a single BC. Here, we used a novel approach to achieve this goal to assess and isolate the retinal pathway that mediates lateral inhibition to an identified BC terminal. We recorded responses to full-field illumination in axotomized BC terminals embedded in goldfish retinal slices, in which visual information could only reach the BC terminal via the lateral inhibitory pathway (see Fig. 1*A*). We found that both rods and cones contributed to the lateral IPSCs (L-IPSCs) targeting Mb terminals during the illumination ("ON" inhibition), while L-IPSCs after the termination of light ("OFF" inhibition) were mediated primarily by a cone-driven retinal cir-

Received June 12, 2011; revised Aug. 29, 2011; accepted Sept. 17, 2011.

Author contributions: J.V. and H.v.G. designed research; J.V. and E.V. performed research; J.V., E.V., and H.v.G. analyzed data; J.V., E.V., and H.v.G. wrote the paper.

This research was funded by NIH-National Eye Institute Grants EY014043 (to H.v.G.) and EY019051 (to J.V.). We thank W. Rowland Taylor and Paul Witkovsky for instructive discussions.

Correspondence should be addressed to Jozsef Vigh, Department of Biomedical Sciences, Colorado State University, Ft. Collins, Colorado 80523. E-mail: jozsef.vigh@colostate.edu.

DOI:10.1523/JNEUROSCI.2959-11.2011

 0270-6474/11/3115884-10$15.00/0

cuit. The L-IPSCs were GABAergic, involving both $GABA_A$ receptors ($GABA_A$Rs) and $GABA_C$ receptors ($GABA_C$Rs), much like reciprocal feedback at Mb terminals (Vigh and von Gersdorff, 2005). However, we show here that the ACs that mediate lateral IPSCs are distinct from those involved in reciprocal feedback.

Our study suggests that, in addition to reciprocal feedback, at least two distinct lateral circuits control the glutamate output of Mb BCs. Furthermore, we show that these circuits operate across a broad range of physiological light conditions.

Materials and Methods

Retinal slice preparation. Living retinal slices were prepared from the retina of goldfish (*Carassius auratus*) of either sex, as described previously (Palmer et al., 2003), except that all procedures were performed under infrared illumination with the aid of PVS-7 Night Vision Goggles and OWL Night Vision Scopes (both from BE Meyers) mounted on Olympus SZ51 stereoscopes to maintain the retina in a fully dark-adapted state. In some cases, parts of the dissection were performed under dim red light. Slices (200–250 μm thick) were superfused at 2–5 ml/min with a Ringer's solution containing the following (in mM): 100 NaCl, 2.5 KCl, 1.0 $MgCl_2$, 2.5 $CaCl_2$, 25 $NaHCO_3$, 0–0.2 ascorbic acid, and 12 glucose, pH 7.45 (osmolarity: 260 ± 2 mOsm, and set with NaOH). The Ringer's solution was gassed continuously with 95% O_2 and 5% CO_2. Drugs were bath applied in the perfusing medium. NBQX, CNQX, (*S*)-(+)-a-amino-4-carboxy-2-methylbenzeneacetic acid (LY367385), 6-imino-3-(4-methoxyphenyl)-1(6*H*)-pyridazinebutanoic acid (SR95531), 3-((R)-2-carboxypiperazin-4-yl)-propyl-1-phosphonic acid [(R)-CPP], and D-AP5 were obtained from Tocris Bioscience. Tetrodotoxin (TTX) was obtained from Alomone Laboratories. All other chemicals and salts were obtained from Sigma.

Electrophysiology and light stimulation. Giant terminals of Mbs with severed axons were identified in the inner plexiform layer (IPL) based on (1) Mb-shaped (bulbous) terminal morphology, (2) single-exponential membrane time constant, and (3) the presence of an L-type Ca^{2+} current and ΔC_m jump in response to depolarization. Axotomized bipolar cell terminals in retinal slices were voltage-clamped in whole-cell mode using a HEKA Elektronik EPC-10 USB patch-clamp amplifier in conjunction with Patchmaster software (version 2.30) or an EPC-9 double patch-clamp amplifier controlled by Pulse software. With either amplifier, the Sine+DC technique was used for real-time measurements of membrane capacitance, in which a 1 kHz sinusoidal voltage command (20–30 mV peak to peak) was added to the holding potential of −60 mV, and the resulting current was analyzed at two orthogonal phase angles by the lock-in amplifier (Gillis, 2000). Recordings were obtained using 6–12 MΩ patch pipettes pulled from 1.5-mm-diameter thick-walled borosilicate glass (World Precision Instruments) on a horizontal puller (model P-97, Sutter), coated with dental wax (Cavex) to reduce pipette capacitance, and filled with solution containing the following (in mM): 95 Cs-gluconate, 25 HEPES, 10 TEA-Cl, 3 Mg-ATP, 0.5 Na-GTP, and 2 EGTA, adjusted to pH 7.2 with CsOH. In addition, methylamine HCl (10 mM) was included to buffer vesicular pH (Cousin and Nicholls, 1997; Vigh et al., 2005). In some cases, 10 methylamine HCl was left out and 95 Cs-gluconate was replaced with a combination of 60 Cs-gluconate and 40 CsCl to increase the amplitude of IPSCs at the holding potential of −60 mV. Some internal solutions contained 3 mM ascorbic acid and/or 3 mM reduced glutathione.

Voltage-clamp series resistance (R_s) errors were not electronically compensated, and liquid junction potential was not corrected. Cells with uncompensated $R_s > 30$ MΩ (or leak of >50 pA at a holding potential of −60 mV) were excluded from further evaluation. Recordings were performed at room temperature and in the day time (morning/afternoon) to avoid circadian changes in transmitter release from bipolar cells (Hull et al., 2006).

Full-field light stimulation of retinal slices was performed with white (Allied Electronics), 505 nm (green), or 660 nm (red) LEDs (American Bright Optoelectronics), positioned 3 cm above the preparation at a 30° angle. The intensities of 505 and 660 nm light pulses were reliably controlled by the command voltage from the EPC-10 digital-to-analog (D/A) output with millivolt precision. In our stimulus range, the number of emitted photons was between 6.6×10^9 and 1.9×10^{12} cm^{-2} s^{-1} ($\lambda = 505$ nm) and between 8.7×10^8 and 2.0×10^{12} cm^{-2} s^{-1} ($\lambda = 660$ nm) as calibrated by an Optical Meter (model 1918-C) equipped with a low-intensity sensor (model 918D-SL-OD3) (both from Newport).

For white light stimulation, slices were stimulated with a white LED connected via soldered wire and BNC cable to a D/A output of the HEKA Elektronik EPC-9 patch-clamp amplifier. Full-field light flashes were delivered by application of 400–500 ms voltage steps from 0 to 5 V. The full dynamic range of LED light intensity was evoked by voltage steps between 2.5 and 5 V, which evoked photon flux between 1.06×10^{11} and 7.32×10^{13} photons cm^{-2} s^{-1}. The timing and amplitude of voltage steps was controlled from within the Pulse Software (HEKA Elektronik) controlling the EPC-9 amplifier. Calibration of light flash timing (onset and offset) was performed with a photodiode connected to the EPC-9 amplifier through an ITHACO 4302 dual 24 dB Octave Filter. Light flash onset and offset had rise and decay time constants of 0.12 and 6.3 ms, respectively. Onset and offset times did not vary as a function of flash duration between 100 and 1000 ms. Calibration of white light intensity was performed with an ILT-1700 photometer and SE033 detector from International Light Technologies. Factory calibration determined the photic illuminance response sensitivity of the detector to be 2.60×10^{-8} A (square feet) (lm^{-1}) or 2.415×10^{-9} A (lux^{-1}), assuming a 3215 K color temperature.

Data analysis. Off-line data analysis was performed using IgorPro software (version 5.03; Wavemetrics). Because light-evoked lateral feedback responses showed a degree of variability from stimulus to stimulus, we presented averaged traces of a minimum of five individual light responses throughout the article, unless otherwise noted. Consecutive light stimulations were applied with a stimulus interval of at least 30 s. Quantification of light responses was performed by integrating the charge (Q) transfer of light-evoked, L-IPSCs for 500 ms (or 400 ms) during the illumination (ON) and for 500 ms (or 300 ms) after the termination of the stimulus (OFF). Reciprocal feedback was quantified by integrating the total current during a 100 ms depolarization from −60 to −20 or 0 mV. This method provides a quick measure of the net charge transfer associated with Ca^{2+} influx (I_{Ca}) plus the reciprocal GABAergic feedback that can be compared across subsequent depolarizations, and has been used previously to quantify relative changes in reciprocal feedback in the absence of I_{Ca} rundown (Vigh et al., 2005). When appropriate, experiments were performed in the presence of LY367385 to avoid reciprocal feedback potentiation due to AC mGluR1 activation (Vigh et al., 2005). Statistics were calculated using SigmaPlot (version 11; Systat Software). Paired or unpaired two-tailed Student's t tests were used to compare datasets. Multiple sets of data were compared using ANOVA (Holm–Sidiak method) or the Mann–Whitney U test, when appropriate. Data were reported as mean ± SEM. Statistics were performed on averaged traces, unless otherwise noted.

Results

Light evokes both ON and OFF lateral IPSCs in single bipolar cell terminals

Whole-cell voltage-clamp recordings were made from Mb terminals in a goldfish retinal slice preparation. These large, bulbous structures are located in the ON sublamina of the IPL, close to the GC layer. It is possible to make whole-cell voltage-clamp recordings from a single axotomized Mb terminal (Palmer et al., 2003). This technique offers several advantages from a biophysical standpoint. For example, axotomized terminals allow accurate recording of membrane capacitance increases (ΔC_m) associated with exocytosis (von Gersdorff and Matthews, 1999). It also allows isolation of reciprocal inhibitory feedback, which is observed in different types of bipolar cells (Dong and Werblin, 1998; Protti and Llano, 1998; Hartveit, 1999; Vigh and von Gersdorff, 2005). In the present study, another advantage of this preparation was exploited: severing the connection between the axon

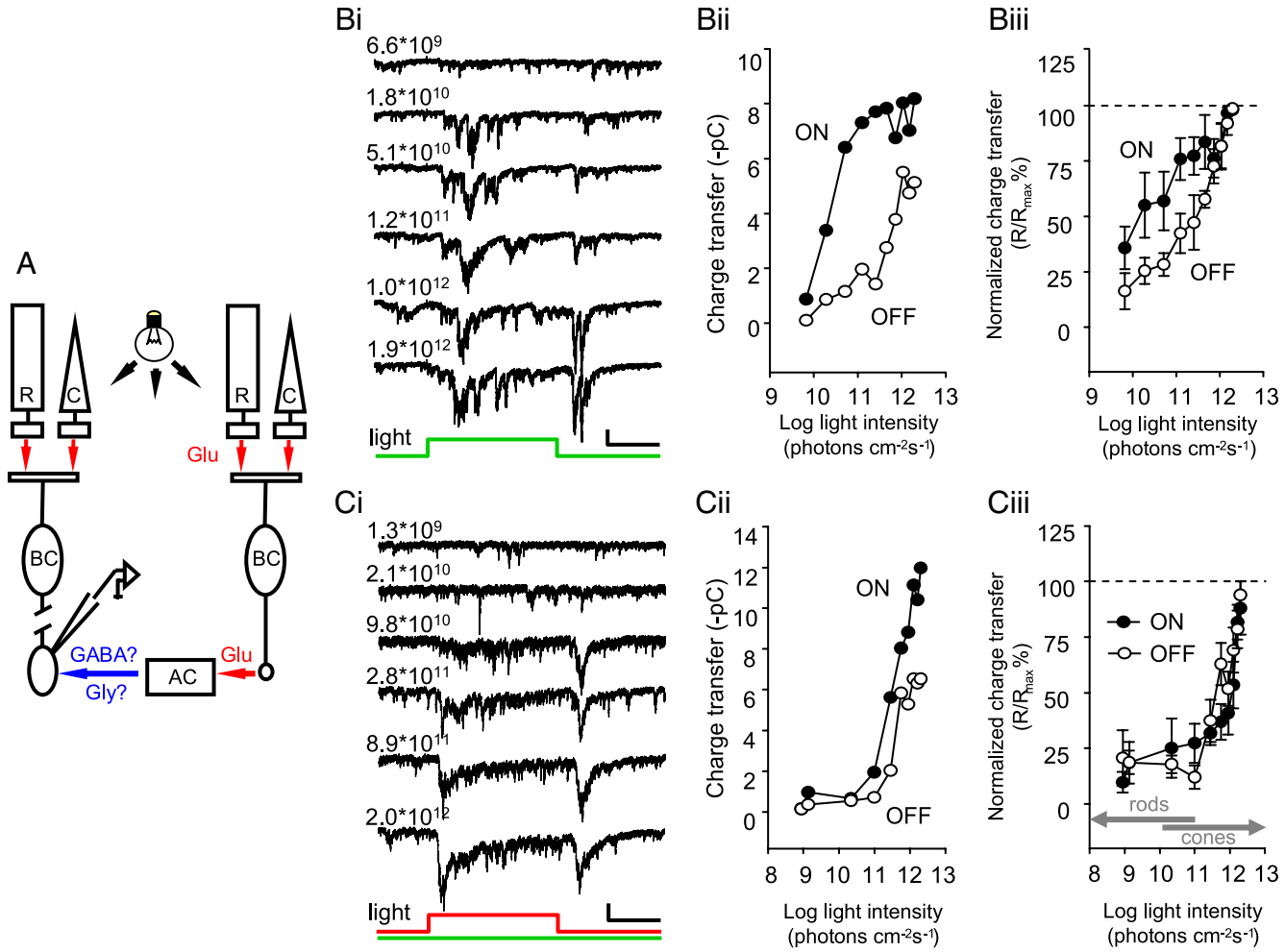

Figure 1. Both rod and cone signals are represented in the L-IPSCs of axotomized Mb terminals. ***A***, Retinal pathway underlying L-IPSCs in axotomized Mb terminals. In the absence of direct visual input from the soma, a light signal can reach axotomized Mb terminals via the lateral inhibitory pathway. R, Rod; C, cone; Gly, glycine; Glu, glutamate. ***Bi***, Representative light-evoked signals recorded from an axotomized Mb terminal. Averaged traces are shown ($n = 3$). Light pulses (500 ms, $\lambda = 505$ nm) were delivered once every 30 s. Intensity of light pulses is given as number of photons ($cm^{-2}\,s^{-1}$), indicated at the top of each trace. Note that ON L-IPSCs first develop at much lower intensities than OFF L-IPSCs. Calibration: 10 pA (vertical), 100 ms (horizontal). ***Bii***, Quantification of L-IPSCs with response–intensity curve (Q/I) for the same experiment shown in ***Bi***. Note that our protocol consisted of flashes at 10 light intensities but only 6 are shown on ***Bi*** for clarity. Charge transfer was calculated by integrating the area under the current trace for 500 ms during the illumination (ON), as well as for 500 ms immediately following the offset of illumination (OFF). Charge values for each trace were plotted against the light intensity on a logarithmic scale. ***Biii***, Summary response/intensity diagram ($n = 5$) obtained with green light flashes (500 ms, $\lambda =$ 505 nm). R/R_{max} percentage calculation was performed for each cell before averaging values across cells at any given intensity. Error bars represent ±SE. Note that sizeable ON responses were present at the lowest intensities applied in this study (in the high end of the rod sensitivity range), at intensities where OFF L-IPSCs were barely present. Also, ON L-IPSCs were nearly saturated at rod-saturating intensities. Both of these observations support the notion that ON L-IPSCs are rod dominant, whereas OFF L-IPSCs are cone dominant. The difference between the ON and OFF datasets was statistically significant ($p < 0.001$, ANOVA, Holm–Sidak method). ***Ci***, Representative light-evoked signals recorded from an axotomized Mb terminal. Averaged traces are shown ($n = 2$–4). Light pulses (500 ms, $\lambda = 660$ nm) were delivered once every 30 s, superimposed on a steady background ($\lambda = 505$ nm). Intensity of light pulses is given as the number of photons ($cm^{-2}\,s^{-1}$), indicated at the top of each trace. The intensity of the green background light was 10^{10} photons $cm^{-2}\,s^{-1}$. Note that both ON and OFF L-IPSCs were present, and that they developed at the same bright intensities. Calibration: 10 pA (vertical), 100 ms (horizontal). ***Cii***, Quantification of L-IPSCs with Q/I curve for the experiment shown in ***Ci***. Charge transfer was calculated as in ***Bii***. ***Ciii***, Summary response/intensity diagram ($n = 5$) obtained with red light flashes (500 ms, $\lambda = 660$ nm) superimposed on a steady green background ($\lambda = 505$ nm). Data are presented as in ***Biii***. Note that in the presence of (rod-saturating) background light the ON and OFF Q/I curves overlap, and there was no statistical difference between the ON and OFF datasets ($p = 0.209$, ANOVA, Holm–Sidak method).

terminal and somatodendritic compartment of the BC results in light-evoked membrane currents of the terminal being exclusively mediated by the AC synapses that provide lateral feedback inputs from ACs to the axotomized terminal (Fig. 1*A*).

Full-field light stimulation ($\lambda = 505$ nm, 500 ms) at increasing intensities triggered L-IPSCs in axotomized terminals voltage-clamped at −60 mV (Fig. 1*Bi*). The intensity range of the light stimuli spanned the mesopic light levels (Krizaj, 2000); the dimmest green flash was just below the cone activation threshold, and the intensity of the brightest light step was 1 log unit above rod saturation. Light triggered L-IPSCs during the illumination (ON), as well as after the termination of light stimulus (OFF) (Fig. 1*Bi*). Note that in this representative terminal the second 505 nm flash, which had an intensity ($I = 1.8 \times 10^{10}$) (Fig. 1*Bi*) around the cone threshold (~10^{10} photons $cm^{-2}\,s^{-1}$) (Busskamp et al., 2010) evoked large ON, but only tiny OFF L-IPSCs. In the mouse retina, the rod pigment's sensitivity to 500 nm light is nearly 2 log units higher than that of the medium-wavelength cone pigment, and ~4 log units higher than that of the short-wavelength cone pigment (Lyubarsky et al., 1999). Although the spectral sensitivity of goldfish rods and cones (Palacios et al., 1998) are somewhat different from those of the mouse, this finding suggested that in Mb terminals ON L-IPSCs received larger rod input than OFF L-IPSCs.

The L-IPSCs were quantified as inhibitory *Q* transfer (see Materials and Methods) to generate intensity–response curves for both the ON and OFF components (Fig. 1*Bii*). Importantly, the quantification revealed that amplitudes of ON L-IPSCs appeared to plateau at the light intensities known to saturate rods ($\sim 10^{11}$ photons cm^{-2} s^{-1}). On the other hand, the intensity–response curve of OFF L-IPSCs did not saturate but rather increased linearly across the range of our (green) light intensities.

We found a large variation in the amplitude of light-evoked L-IPSCs from terminal to terminal. This variation might be physiologically relevant: it is possible that the number of lateral inputs is different across Mb terminals. Nonetheless, we cannot exclude the possibility that this variation was also caused by the slicing procedure, which may have destroyed a variable portion of long, wide-field AC processes targeting the recorded Mb terminal. Despite this variation, it was possible to generate cumulative intensity–response curves by first normalizing L-IPSCs (*R*s) evoked by a range of light intensities from a given terminal by reference to the largest L-IPSC amplitude (R_{max}). Then, the normalized values (R/R_{max} %) corresponding to each of the tested light intensities were averaged across multiple cells (Fig. 1*Biii*). Statistical analysis confirmed that the differences between the normalized ON and OFF intensity/response data were significant (ANOVA, Holm–Sidiak method, $p < 0.001$).

To further examine the possible differences between rod and cone contributions to L-IPSCs, we stimulated the retinal slices with full-field red light flashes ($\lambda = 660$ nm, 500 ms) of increasing intensity (between 8.7×10^8 and 2.0×10^{12} cm^{-2} s^{-1}), superimposed on a steady, rod-saturating 505 nm background ($I = 10^{10}$ cm^{-2} s^{-1}) (Sterling, 2004) that barely stimulated cones. With this steady green background, both ON and OFF L-IPSCs were turned on at around the cone-sensitivity threshold ($\sim 10^{11}$ cm^{-2} s^{-1}) (Fig. 1*Ci*,*Cii*). The intensity–response curves of ON and OFF L-IPSCs triggered by red flashes on the green background ran parallel, and no responses appeared to saturate within our intensity range (Fig. 1*Cii*). There was no statistical difference ($p = 0.209$, ANOVA) between the normalized ON and OFF L-IPSC intensity–response data (Fig. 1*Ciii*). These results indicated that under these conditions both the ON and the OFF L-IPSCs were mediated by cone-driven components.

More importantly, statistical analysis revealed significant difference ($p < 0.001$, Mann–Whitney *U* test) between the distribution of normalized data representing the ON L-IPSCs triggered by a green flash intensity series on a dark background (Fig. 1*Biii*, ON trace) and that of ON L-IPSCs triggered by a red flash intensity series superimposed on rod-saturating green background light (Fig. 1*Ciii*, ON trace), indicating that rods substantially contributed to ON L-IPSCs in the mesopic intensity range. Similar comparison of the corresponding OFF L-IPSC datasets revealed no statistical difference ($p = 0.200$, Mann–Whitney *U* test). Thus, the intensity–response distribution of OFF L-IPSCs was independent of the presence of background light. In other words, the rod-saturating background illumination did not alter the sensitivity of OFF L-IPSCs (despite the change in wavelength of the stimulating light flashes) but reduced the sensitivity of ON L-IPSCs by ~1 log unit (Fig. 1, compare *Biii*, *Ciii*, cumulative ON traces).

In summary, our data suggest that both ON and OFF L-IPSCs at Mb axon terminals receive mixed rod and cone input. However, the relative contribution of rods and cones to ON and OFF L-IPSCs is uneven. In the mesopic light intensity range, ON L-IPSCs receive large rod- and cone-driven input, whereas the OFF L-IPSCs are primarily driven by cones.

Differential contribution of ON and OFF retinal pathways to lateral feedback

The separation of light information into ON and OFF pathways, initially encoded as photoreceptor hyperpolarization, is accomplished by the existence of heterogeneous glutamate receptor populations in ON and OFF BCs, which depolarize and hyperpolarize in response to light, respectively. The retinal ON signaling pathway begins with a group III mGluR, sensitive to L-AP4, a group III mGluR agonist (Slaughter and Miller, 1981). Indeed, L-AP4 (10–20 μM) significantly reduced the ON L-IPSCs in Mb terminals (Fig. 2*Ai*,*Aii*) (to 23 ± 3% of control; $n = 5$; $p < 0.02$, paired Student's *t* test, two-tailed) confirming that ON BCs provide excitatory input to the ACs that mediate light-evoked ON L-IPSCs. L-AP4 also tended to reduce OFF L-IPSCs (to 29 ± 5% of control; $n = 5$; $p < 0.13$, NS, paired Student's *t* test, two-tailed) (Fig. 2*Ai*,*Aii*,*D*), although this effect was not significant. The L-AP4 effect on OFF L-IPSCs might be related to the presynaptic inhibitory effect of group III mGluRs on OFF BCs (Awatramani and Slaughter, 2001), which would reduce excitation of the ACs that mediate OFF L-IPSCs in Mb terminals. In addition, L-AP4 might affect ACs via group III mGluRs directly (Brandstätter et al., 1996; Koulen et al., 1996).

OFF BCs use ionotropic AMPA receptors (AMPARs) and KA receptors (KARs) to detect glutamate efflux from photoreceptors. Application of the AMPAR/KAR antagonist NBQX (10 μM) markedly reduced the OFF L-IPSCs (to 30 ± 6% of control; $n = 10$; $p < 0.0001$, paired Student's *t* test, two tailed). Light responses of ACs are mediated by AMPARs and NMDA receptors (NMDARs) (Dixon and Copenhagen, 1992), with AMPARs thought to be more critical for transient ACs (Matsui et al., 2001; Vigh and Witkovsky, 2004). Therefore, the NBQX effect on OFF L-IPSCs might also have been caused by inhibition the OFF BC → AC synapse. By the same token, it was our expectation that NBQX would eliminate or reduce light-evoked ON L-IPSCs by blocking the ON BC → AC synapse. Surprisingly, the opposite was observed: NBQX increased the ON L-IPSCs (Fig. 2*Bi*,*Bii*,*D*) (to 168 ± 30% of control; $n = 10$; $p < 0.03$, paired Student's *t* test, two tailed). The fact that NBQX did not block the ON BC → AC synapse suggests that glutamatergic receptors other than AMPAR/KARs, perhaps NMDARs, not only contributed to glutamatergic synaptic transmission, but were also able to independently carry the visual information after pharmacological block of AMPARs/KARs. To test this notion, we first applied NBQX (10 μM) with the NMDAR antagonist D-AP5 (50 μM). This cocktail markedly reduced both ON and OFF L-IPSCs [to 12 ± 3% of control ($p < 0.03$) and 24 ± 10% of control ($p < 0.03$), respectively; $n = 5$] (Fig. 2*D*). Application of D-AP5 (50 μM) alone also reduced both the ON and the OFF L-IPSCs [to 33 ± 8% of control ($p < 0.05$) and 65 ± 14% of control ($p = 0.3$, NS), respectively; $n = 4$]. Similar results were obtained when we used another selective NMDAR antagonist, (R)-CPP. When (R)-CPP (20 μM) was applied together with NBQX (10 μM), the cocktail reduced both the ON and OFF L-IPSCs [to 6 ± 2% of control ($p < 0.04$) and 15 ± 8% of control ($p < 0.04$), respectively, $n = 6$] (Fig. 2*Ci*,*Cii*,*D*). Like D-AP5, (R)-CPP (20 μM) alone reduced both the ON and the OFF L-IPSCs [to 55 ± 18% of control ($p = 0.1$, NS) and 47 ± 8% of control ($p < 0.03$), respectively; $n = 4$]. These results indicated that NMDARs contribute significantly to synaptic transmission between BCs and ACs that mediate lateral inhibition to Mb terminals (Fig. 2*D*). The partial inhibition of L-IPSCs by D-AP5 alone also suggests that AMPARs/KARs are present at both the ON BC → AC and OFF BC → AC synapses.

It is tempting to speculate that NBQX-evoked enhancement of ON L-IPSCs in Mb terminals might be mediated by horizontal

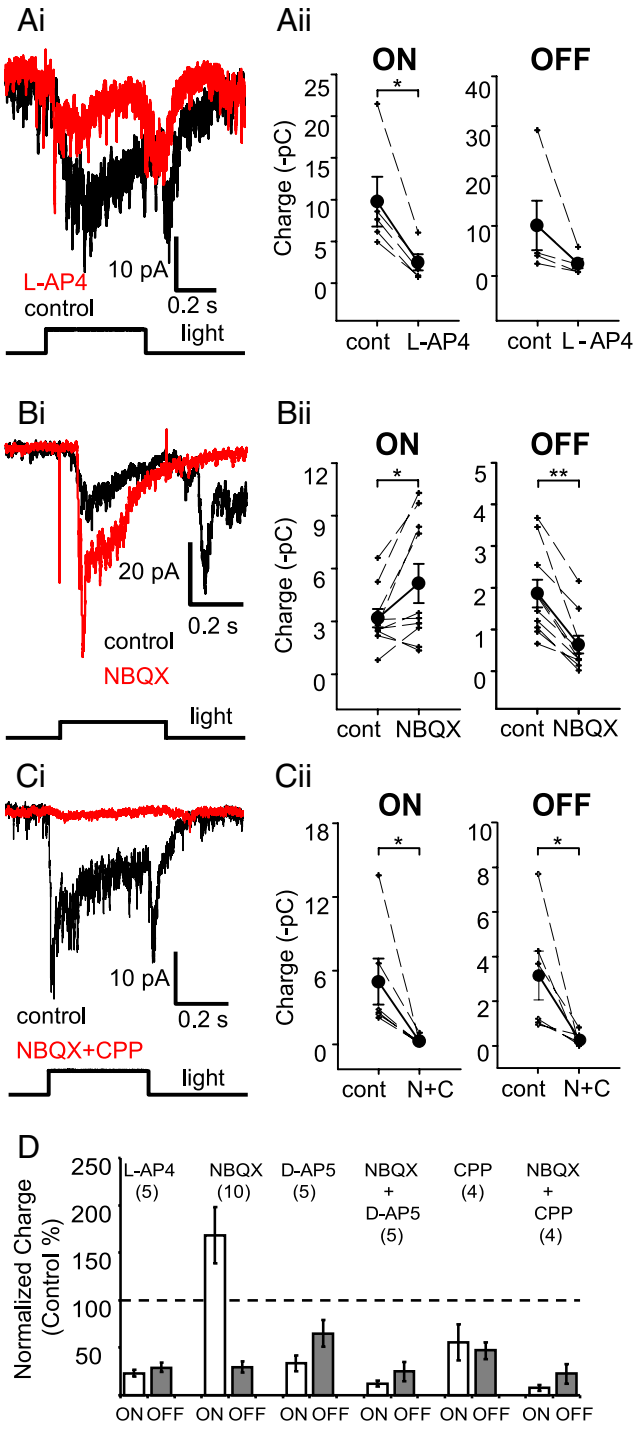

Figure 2. ON and OFF retinal pathways contribute to light-evoked lateral feedback at Mb bipolar terminals. ***Ai***, Both the ON and the OFF portions of light-evoked ($\lambda = 505$ nm, $I = 1.95 \times 10^{12}$ photons cm^{-2} s^{-1}, 500 ms) L-IPSCs were reduced by the group III mGluR agonist L-AP4 (10–20 μM, red trace). Average traces are shown for each condition ($n = 5$). ***Aii***, Quantification of the effect of L-AP4 on the ON and OFF L-IPSC charge transfers. L-AP4 significantly reduced ON L-IPSC charge (*$p < 0.02$, paired Student's *t* test, two tailed), but the reduction of OFF L-IPSCs was not significant ($p < 0.13$, paired Student's *t* test, two tailed). Measurements, analysis, and presentation of drug effects on L-IPSCs are performed this way throughout the article. ***Bi***, The AMPAR/KAR antagonist NBQX (10 μM, red trace) substantially reduced the OFF L-IPSCs evoked by bright white light (400 ms, $I = 7.32 \times 10^{13}$ photons cm^{-2} s^{-1}), but markedly increased the ON L-IPSCs. ***Bii***, Quantification of the NBQX effect on ON and OFF L-IPSC charge transfers. NBQX significantly reduced the OFF L-IPSCs (**$p < 0.0001$, paired Student's *t* test, two-tailed), and significantly enhanced the ON L-IPSCs (*$p < 0.03$, paired Student's *t* test, two-tailed). ***Ci***, L-IPSCs were essentially eliminated by the combination of ionotropic glutamate receptor antagonists NBQX (AMPAR/KAR, 10 μM) and (*R*)-CPP (NMDAR, 20 μM) (red trace). ***Cii***, Quantification of the effect of combined ionotropic glutamate receptor antagonists [NBQX + (*R*)-CPP, N+C) on the ON and OFF L-IPSCs. (R)-CPP + NBQX significantly reduced both the ON and OFF components of the red light ($\lambda = 660$ nm, 500 ms, $I = 2.02 \times 10^{12}$ photons cm^{-2} s^{-1}) evoked the L-IPSC charge (*$p < 0.05$, paired Student's *t* test). ***D***, Summary diagram of normalized effects of pharmacological agents affecting retinal glutamatergic signaling on light-evoked L-IPSCs. Data are presented as mean ± SE.

cells (HCs) in the outer retina. For example, an AMPAR/KAR antagonist will hyperpolarize HCs (Krizaj et al., 1994), removing the HC feedback to photoreceptors (Hirasawa and Kaneko, 2003; Fahrenfort et al., 2005, 2009; Tatsukawa et al., 2005; Davenport et al., 2008; Thoreson et al., 2008) and, if present in the goldfish retina, the GABAergic feedforward inhibition from HCs to ON BCs (Duebel et al., 2006). The resulting disinhibition would increase the light-evoked excitation of ACs by ON BCs via NMDARs, leading to larger ON L-IPSCs at the Mb terminals.

GABAergic amacrine cells mediate lateral inhibition to Mb terminals

$GABA_A$Rs and $GABA_C$Rs are expressed to different degrees in different types of bipolar cells (Wässle et al., 1998; McCall et al., 2002). In previous studies, we found that reciprocal feedback at Mb terminals is mediated by both ionotropic $GABA_A$ and $GABA_C$ receptors, with $GABA_C$ receptors responsible for sustained inhibition (Vigh and von Gersdorff, 2005). In retinas of other species, $GABA_C$Rs, also located primarily on ON BCs, primarily influence the ON pathway (Zhang and Slaughter, 1995; Eggers and Lukasiewicz, 2006). Lateral inhibition to rod BCs in the rat retina, triggered by focal pharmacological activation of ON BCs, was also mediated by $GABA_C$Rs (Chávez et al., 2010). We found that light-evoked lateral feedback IPSCs were reduced by the $GABA_C$R antagonist 1,2,5,6-tetrahydropyridin-4-yl-methylphosphonic acid (TPMPA) [100–150 μM, ON: to 42 ± 10% of control response ($p < 0.04$); OFF: to 68 ± 8% of control response ($p < 0.02$); $n = 5$] (Fig. 3*Ai*,*Aii*,*C*).

The specific $GABA_A$R antagonist SR95531 (25 μM) markedly increased both components of lateral feedback (ON: to 174 ± 15% of control response, $p < 0.02$; OFF: to 233 ± 41% of control response, $p < 0.05$; $n = 7$) (Fig. 3*Bi*,*Bii*,*C*). Similar effects have been described in the inner retina, in that $GABA_A$R blockers, such as the SR95531, not only block the $GABA_A$Rs on the (Mb) BC axon terminals, but also eliminate $GABA_A$R-mediated serial inhibition between ACs (Zhang et al., 1997; Eggers and Lukasiewicz, 2010). This effect on serial inhibition is especially pronounced following full-field illumination. As a result, the presynaptic ACs providing lateral IPSCs (in this case to the Mb terminals) are disinhibited. Subsequent light-evoked excitation of ACs by BCs causes larger GABA release, which in turn acts on $GABA_C$Rs of BCs. In our hands, however, TPMPA (up to 300 μM) reduced but did not completely block SR95531-elevated L-IPSCs (Fig. 3*Biii*, blue trace). Subsequent application of picrotoxin (PTX; 100 μM), a strong blocker of both $GABA_A$Rs and $GABA_C$Rs in the goldfish retina (Vigh et al., 2005), eliminated the remaining lateral feedback IPSCs (Fig. 3*Biii*, green trace). This finding raised the possibility that light-evoked lateral feedback IPSCs might have a glycinergic component, as PTX also inhibits ionotropic glycine receptors in the retina at the concentration we applied (100 μM) (Li and Slaughter, 2007). However, strychnine (1 μM), a specific antagonist of ionotropic glycine receptors in the retina at these low concentrations (Protti et al., 1997), had no significant effect on ON or OFF L-IPSCs [control ON: 2.69 ±

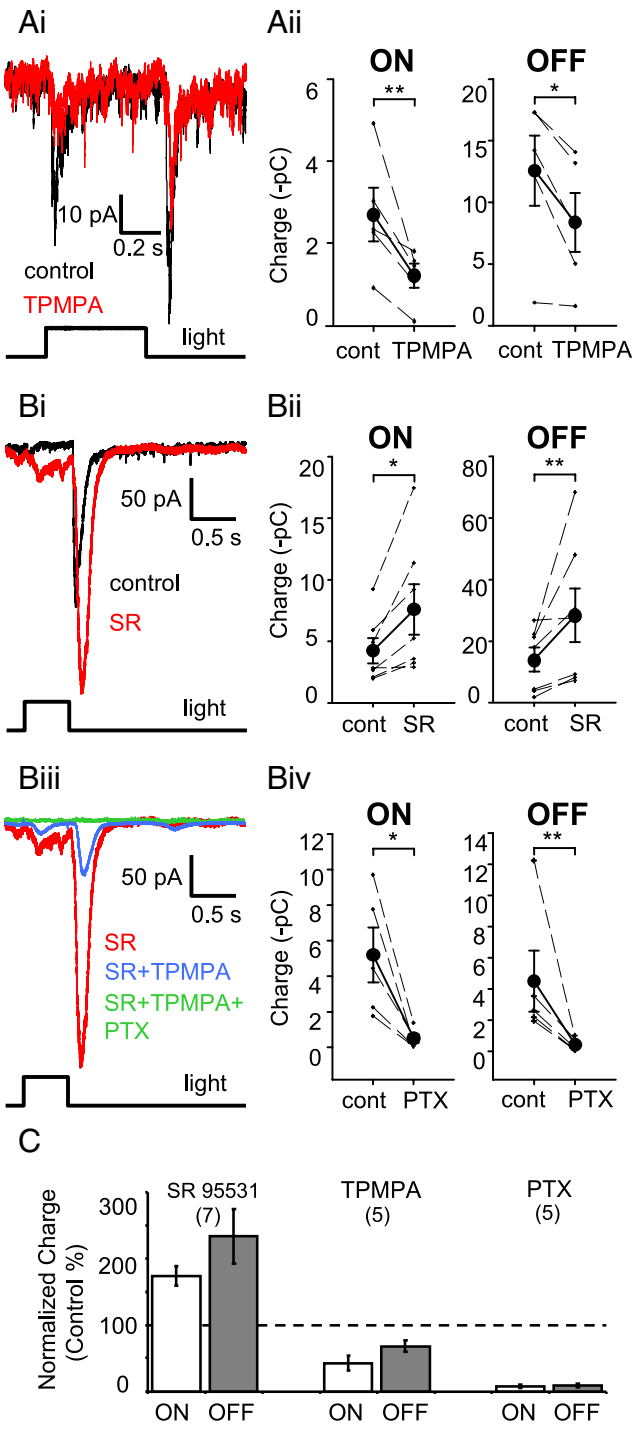

Figure 3. Light-evoked lateral feedback at Mb bipolar terminals is GABAergic. ***Ai***, Both the ON and the OFF portions of the light-evoked ($\lambda = 505$ nm, $I = 1.95 \times 10^{12}$ photons cm^{-2} s^{-1}, 500 ms) L-IPSCs were inhibited by the GABA$_C$R antagonist TPMPA (150 μM, red trace). Average traces are shown for each condition ($n = 5$). ***Aii***, Quantification of the effect of TPMPA on ON and OFF charge transfers of L-IPSCs. Means are shown as filled circles connected with solid black lines. Error bars represent ±SE. TPMPA significantly reduced the charge of both ON and OFF L-IPSCs (*$p < 0.05$, **$p < 0.02$, paired Student's *t* test, two tailed). ***Bi***, SR95531 (25 μM, SR, red trace) a GABA$_A$R antagonist markedly increased L-IPSCs, indicating that ACs providing GABAergic feedback to Mb terminals receive serial inhibition via GABA$_A$ receptors. ***Bii***, Quantification of the effect of SR95531 on ON and OFF charge transfers of L-IPSCs. SR95531 significantly increased the charge of both ON and OFF L-IPSCs (*$p < 0.05$, **$p < 0.02$, paired Student's *t* test, two tailed). ***Biii***, Same cell as in ***Bi***; traces obtained by consecutive treatments are divided into two panels for increased visibility. The SR95531-elevated L-IPSCs (SR, red trace) were reduced by TPMPA (here 300 μM shown, blue trace) but were not eliminated completely. Complete L-IPSC block of SR95531-elevated L-IPSCs could be achieved upon addition of PTX (100 μM, green trace). ***Biv***, Quantification of PTX effect on the ON and OFF charge transfer of L-IPSCs. PTX significantly decreased the charge of both ON and OFF L-IPSCs (*$p < 0.05$, **$p < 0.02$, paired Student's *t* test, two tailed). ***C***, Summary diagram of normalized GABAergic drug effects on light-evoked L-IPSCs. Data are presented as mean ± SE.

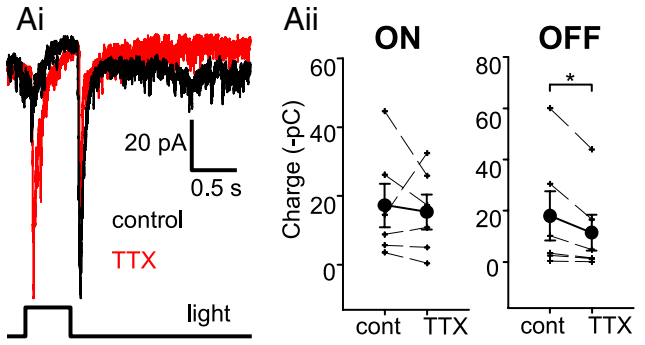

Figure 4. The propagation of GABAergic lateral feedback signals targeting Mb bipolar terminals involves TTX-sensitive mechanisms. ***Ai***, Both the ON and OFF portions of the light-evoked ($\lambda = 505$ nm, $I = 1.95 \times 10^{12}$ photons cm^{-2} s^{-1}, 500 ms) L-IPSCs are affected by TTX, albeit differently. The example shown here depicts a cell in which the ON L-IPSCs were increased, whereas the OFF L-IPSCs were suppressed by TTX (2 μM, red trace). Average traces are shown for each condition ($n = 5$). ***Aii***, Quantification of the TTX effect on the ON and OFF L-IPSC charge transfer ($n = 6$). TTX significantly reduced the charge of OFF L-IPSCs (*$p < 0.03$, paired Student's *t* test), but the effect of TTX on ON L-IPSCs was not significant ($p < 0.72$, paired Student's *t* test). Note that TTX reduced ON L-IPSCs in three of six cells tested, and increased ON L-IPSCs in the other three of six cells.

0.40 pC; strychnine ON: 3.34 ± 0.52 pC ($p = 0.38$, $n = 3$); control OFF: 1.36 ± 0.09 pC; strychnine OFF: 1.44 ± 0.10 pC ($p = 0.71$, $n = 3$); data not shown], consistent with the finding that spontaneous IPSCs recorded from Mb terminals were eliminated by TPMPA and SR95531 (Vigh et al., 2005). Therefore, it is most likely that the incomplete block of L-IPSCs by TPMPA in the presence of SR95531 resulted from an abnormally high synaptic GABA concentration. In other words, it is likely that full-field stimulation of the entire disinhibited AC network released large amounts of GABA, and that the competitive antagonist TPMPA was unable to block all GABA$_C$Rs.

GABAergic lateral inhibition is TTX sensitive

TTX-sensitive voltage-gated sodium (Na$_V$) channels are known to mediate long-range dendritic signaling of wide-field ACs (Cook and McReynolds, 1998; Shields and Lukasiewicz, 2003), which are GABAergic (Masland and Raviola, 2000). TTX-sensitive, wide-field GABAergic ACs were found to contribute to surround responses of some ganglion cells (Taylor, 1999; Flores-Herr et al., 2001) and to mediate lateral feedback to rod BCs (Chávez et al., 2010). TTX-sensitive Na$_v$ channels are also present in the somatodendritic compartment of a subpopulation of cone BCs in the goldfish retina, producing a small, rapidly inactivating current (Zenisek et al., 2001).

In our experiments, TTX (1–2 μM) consistently reduced the OFF lateral IPSCs in each cell (to 44 ± 10% of control response, $p < 0.03$, $n = 6$). These data suggest that Na$_v$ channels in OFF cone BCs in the goldfish retina could be functionally significant and/or that TTX-sensitive Na$_v$ channels are capable of boosting OFF lateral inhibition in OFF ACs presynaptic to Mb terminals.

However, TTX effects on the ON lateral IPSCs were mixed, with inhibition in three of six cells and enhancement in three of six cells (Fig. 4*Ai*,*Aii*). The TTX-evoked enhancement of ON L-IPSCs is interesting, because it suggests that the ON GABAergic

←

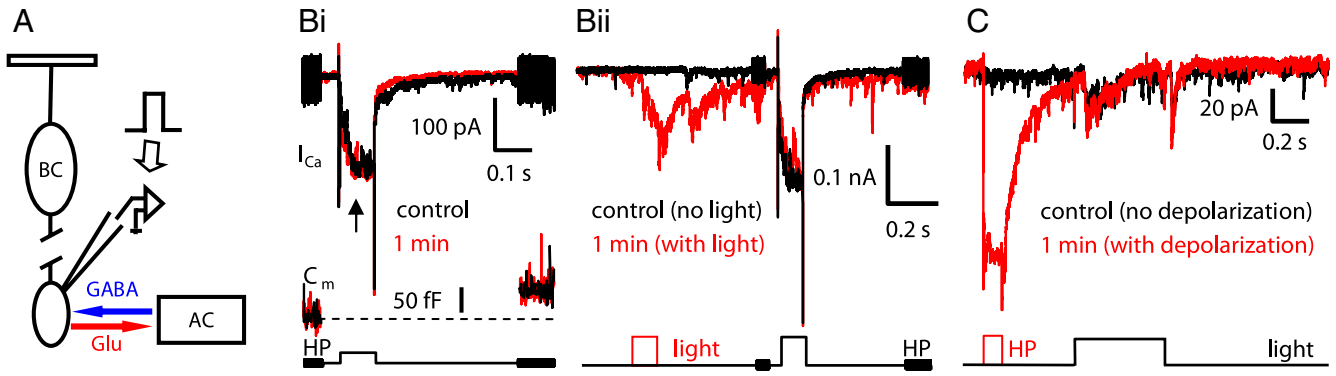

Figure 5. GABAergic lateral and reciprocal feedback to Mb axon terminals are mediated by separate populations of ACs. ***A***, Diagram depicting exclusive triggering of reciprocal feedback by direct step depolarization of an axotomized Mb terminal. ***Bi***, Depolarization of an axotomized Mb terminal from the holding potential (HP) of −60 to 0 mV for 100 ms activated calcium influx through voltage-gated calcium channels (I_{Ca}), which triggered glutamate release, as evidenced by a jump in ΔC_m. The protocol used is shown in the bottom trace. The fast voltage sinewave used to measure C_m was not delivered during the depolarization. The inhibitory feedback to the presynaptic terminal is expressed as a flurry of outward IPSCs superimposed on I_{Ca} (arrow). Experiments were performed in the presence of LY367385 (100 μM) to block mGluR1-dependent potentiation of reciprocal feedback. Under these conditions, consecutive depolarizations of the presynaptic terminal 1 min apart produced reciprocal feedback with similar magnitudes. There was no evidence of short-term depression (red trace). The resting C_m for this terminal was 5.5 pF. ***Bii***: Same cell as in ***Bi***. A light stimulus was applied ($\lambda = 505$ nm, $I = 1.95 \times 10^{12}$ photons cm^{-2}s^{-1}, 100 ms) to evoke pure lateral feedback between two reciprocal feedback steps (1 min apart), such that the light-evoked L-IPSCs preceded the second presynaptic depolarizations by 500 ms. However, the amplitude of reciprocal feedback did not decrease. ***C***, The reverse of the experiment depicted in ***Bii***. Consecutive, bright white light-evoked ($I = 7.32 \times 10^{13}$ photons cm^{-2}s^{-1}) L-IPSCs were triggered 1 min apart, but a 100 ms depolarization from −60 to 0 mV was delivered to the Mb terminal 300 ms before the second light pulse (red trace). No differences in the light-evoked L-IPSCs were noted.

ACs presynaptic to the Mb terminals may receive serial GABAergic inhibition (Zhang et al., 1997; Eggers and Lukasiewicz, 2010) that is, at least partially, Na_V channel dependent. This effect was not present all the time, which might be related to the observation that the Na_V channel-possessing ACs are typically large wide-field cells that might have been severed during slice preparation. If these connections are absent, the net TTX effect is inhibitory, implying that TTX-sensitive Na_V channels are capable of boosting the lateral inhibition of ACs presynaptic to the Mb terminals.

Lateral and reciprocal feedback are mediated by separate sets of amacrine cells

Our data demonstrate that lateral feedback inhibition of Mb terminals is accomplished via $GABA_A$Rs and $GABA_C$Rs, in a manner similar to that of reciprocal feedback inhibition (Vigh and von Gersdorff, 2005; Vigh et al., 2005). Reconstructions of synaptic connections to and around Mb axon terminals, based on electron micrographs of ultrathin sections, led to the conclusion that reciprocal BC → AC synapses are physically distinct from AC → BC lateral feedback synapses (Marc and Liu, 2000). However, this systematic morphological study was unable to determine whether or not the same ACs give rise to both types of GABAergic feedback synapses.

The *in situ* axotomized Mb terminal offers the ideal preparation for addressing this question with a physiological approach. First, depolarization of a single Mb terminal will trigger primarily local, reciprocal feedback. This will cause GABA to be released from depolarized AC processes back onto $GABA_A$ and $GABA_C$ receptors on the Mb terminal (Fig. 5*A*). If light-evoked L-IPSCs and reciprocal IPSCs are mediated by the same population of AC processes, activation of reciprocal feedback immediately following light-evoked L-IPSCs, or vice versa, should result in depressed reciprocal (or lateral) inhibition, due to synaptic vesicle pool depletion in ACs and/or desensitization of $GABA_A$Rs. Depolarization of Mb terminals from a holding potential of −60 to 0 mV, in the presence of a Cs^+-based internal solution (see Materials and Methods), evoked a sustained inward current, associated with I_{Ca}, and triggered glutamate release, as evidenced by ΔC_m. Reciprocal GABAergic feedback to the presynaptic terminal was evident as outward IPSCs superimposed on I_{Ca} (Fig. 5*Bi*, black trace, arrow). In the presence of the mGluR1 antagonist LY367385 (100 μM), which has been shown to block progressive potentiation of reciprocal feedback inhibition (Vigh et al., 2005), consecutive depolarizations of presynaptic Mb terminals need to be applied at least 1 min apart to avoid short-term depression (Fig. 5*Bi*, compare black and red traces). Such short-term depression has been previously shown to be due to depletion of synaptic vesicle pools in the GABAergic ACs that mediate reciprocal feedback (Li et al., 2007).

Application of bright light stimulation to evoke L-IPSCs immediately before the triggering of reciprocal feedback, in an alternating stimulation protocol with triggering of control reciprocal feedback with an intertrace interval of 60 s, did not alter the charge transferred by reciprocal feedback IPSCs (103 ± 7% of control, $p < 0.5$, NS, $n = 6$) (Fig. 5*Bii*). With reverse-order stimulation, L-IPSCs in Mb terminals were evoked by bright full-field light stimulations 1 min apart, with the second light stimulus in each pair preceded by depolarization to trigger reciprocal feedback (Fig. 5*C*). The results of light stimulation following depolarization were consistent with the results of depolarization following light stimulation, in that activation of reciprocal inhibitory synapses did not decrease the charge transfer of light-evoked lateral IPSCs (ON: 111 ± 12% of control, $p = 0.62$, $n = 3$; OFF: 105 ± 7% of control, $p = 0.83$, $n = 3$; unpaired Student's t test, two tailed). The results of these experiments strongly support the idea that light-evoked lateral and reciprocal feedback IPSCs at Mb terminals are mediated by separate populations of ACs.

Discussion

The present investigation dissected the reciprocal and lateral IPSCs that target Mb axon terminals, and studied the light-evoked, lateral IPSCs. The use of various light stimulation intensities, combined using pharmacological tools, allowed us to infer the retinal circuitry underlying L-IPSCs (Fig. 6). The major findings of our investigation were as follows: (1) both rods and cones drive lateral feedback to the Mb terminals, albeit with different temporal properties, and, depending on light intensity, both rods and cones contribute substantially to ON L-IPSCs, whereas OFF L-IPSCs are mediated primarily by cone-driven circuits; (2) different populations of GABAergic ACs mediate ON and OFF L-IPSCs; (3) GABA-

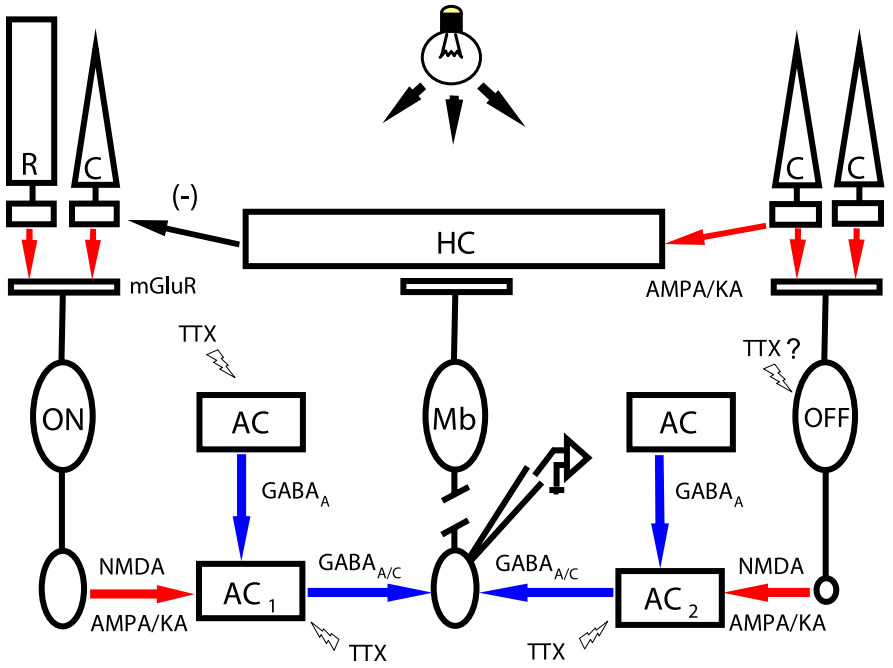

Figure 6. A proposed model for circuitry mediating lateral feedback to the Mb bipolar axon terminal. Light-evoked L-IPSCs in Mb terminals are triggered by at least two distinct retinal circuits, providing inhibition of Mb glutamate release with very different temporal characteristics under scotopic and photopic light conditions. R, Rod; C, cone; RED arrow, glutamatergic synapse; BLUE arrow, GABAergic synapse.

ergic ACs that mediate TTX-sensitive lateral inhibition receive serial GABAergic inhibition from other ACs; (4) $GABA_A$Rs and $GABA_C$Rs contribute to both ON and OFF L-IPSCs; and (5) lateral and reciprocal feedback inhibition to Mbs are mediated by separate populations of GABAergic ACs.

Rod signals are modulated by inner retinal inhibitory feedback

In the mammalian retina under low-scotopic conditions, the majority of rod signals are processed by a dedicated circuitry: the rod → rod BC → AII AC → cone BC → GC pathway (Bloomfield and Dacheux, 2001) is intersected at rod BC terminals by GABAergic reciprocal feedback inhibition from GABAergic A17 ACs (Hartveit, 1999; Zhang et al., 2002; Chávez et al., 2006). The long processes of A17 could potentially carry inhibitory signals over tens to hundreds of micrometers (Menger and Wässle, 2000) and mediate lateral feedback inhibition of distant rod BCs. Nonetheless, the A17 appears to be specialized to provide reciprocal inhibition in a parallel fashion to many rod BCs independently along its processes, instead of participating in spatial (lateral) signaling (Grimes et al., 2010). Rod BCs in the mammalian retina receive lateral inhibition from an as yet unidentified population of GABAergic ACs, which use TTX-sensitive (Na_V) conductances to transfer the signal (Bloomfield and Völgyi, 2007; Chávez et al., 2010). It is not known whether scotopic signals are subject to further modulation by lateral and/or reciprocal feedback inhibition at cone BC terminals, which are the last step on the way toward GCs (DeVries and Baylor, 1995; Field and Chichilnisky, 2007; Gauthier et al., 2009).

In the goldfish retina, Mb BCs carry mixed rod-cone signals (Wong et al., 2005; Joselevitch and Kamermans, 2007) and make direct synapses onto GCs (Arai et al., 2010; Palmer, 2010). Regardless of this fundamental difference between the circuits that mediate scotopic vision in goldfish and mammals, Mb axon terminals are very similar to mammalian rod BCs in that they also receive robust GABAergic reciprocal feedback (Vigh and von Gersdorff, 2005) and, as demonstrated in the present study, lateral feedback. Importantly, the origin of lateral feedback IPSCs that arrive at the Mb axon terminal is consistent with the known inputs to Mb BC dendrites, as both rod- and cone-driven components were found to contribute to light-evoked L-IPSCs (Fig. 1*Biii*,*Ciii*).

ON and OFF pathways interact to mediate lateral feedback, but do not overlap

In the rabbit retina, L-AP4 sensitive, lateral inhibitory ("cancelling") feedback currents in rod BCs, which turn on at the onset of light stimulation, originate from neighboring ON BCs (Molnar and Werblin, 2007). Likewise, lateral feedback IPSCs to rod BCs in the rat retina could be more effectively triggered by pharmacological stimulation of ON BCs than by stimulation of OFF BCs (Chávez et al., 2010). We also recorded L-AP4 sensitive ON L-IPSCs in Mb BCs (Fig. 2*Ai*). The axotomized Mb terminals we recorded from were physically separated from their dendritic trees, where BCs receive excitatory inputs from photoreceptors. Thus, the onset of ON L-IPSCs relative to that of excitatory inputs could not be determined. Cancelling L-IPSCs could contribute to the surround of the Mb receptive field (Saito et al., 1981). If the timing of ON L-IPSCs were slightly delayed relative to light-evoked excitation ("delayed cancelling"), its function would be similar to that of reciprocal feedback, which shortens sustained responses and inhibits low-frequency signal transfer, thereby enhancing propagation of high-frequency or transient stimuli (Molnar and Werblin, 2007). Future experiments involving recordings of light-evoked responses in intact Mb BCs will be needed to clarify these functionally important issues for the vertebrate retina.

We found that L-IPSCs in Mb BCs also have a strong, independent OFF component. Thus, Mb BCs are subject to "ON/OFF crossover inhibition," (Molnar et al., 2009) a configuration in which ACs with OFF responses deliver inhibitory inputs to ON cells, and vice versa. ON/OFF crossover inhibition has been demonstrated at synapses from ACs to GCs (Pang et al., 2007), ACs to ACs (Hsueh et al., 2008), and ACs to BCs (Molnar and Werblin, 2007; Zhang and Wu, 2009).

Glutamatergic EPSCs in GCs following depolarization of presynaptic Mbs are much longer than might be expected based on the duration of presynaptic depolarization, due to the spread of depolarization in the network of presynaptic Mbs coupled by gap junctions (Arai et al., 2010). As this coupling is strongest in the light-adapted retina (Arai et al., 2010), it is tempting to speculate that cone-dominant OFF L-IPSCs (Fig. 1*Bi*) might serve to terminate presynaptic release from Mbs to temporally restrict the glutamate output to the period of light stimulation under photopic conditions.

In this study, we did not fully identify the ACs that evoked L-IPSCs in Mbs. We did, however, identify their GABAergic nature (Fig. 3) and show that they receive serial GABAergic inhibition from other ACs (Dowling and Werblin, 1969) via $GABA_A$Rs (Zhang et al.,

1997; Watanabe et al., 2000; Eggers and Lukasiewicz, 2010). Due to the fact that ON and OFF L-IPSCs were differentially modulated by TTX (i.e., ON L-IPSCs were either reduced or enhanced, while OFF L-IPSCs were reduced, as shown in Fig. 4*Ai*), it is unlikely that a single population of ACs receiving inputs from both ON and OFF BCs mediates all L-IPSCs in Mb BCs. To the contrary, we propose that ON and OFF L-IPSCs may be mediated by two functionally distinct sets of wide-field GABAergic ACs (Fig. 6).

Lateral and reciprocal feedback IPSCs at Mb terminals are mediated by distinct ACs

There are many similarities between the synaptic events that underlie lateral and reciprocal feedback to Mbs (Vigh and von Gersdorff, 2005). The first similarity is that GABAergic ACs receive excitatory glutamatergic input from BCs via AMPA/KA and NMDA receptors in both cases. Interestingly, as seen at the Mb reciprocal feedback synapse, NMDAR activation can trigger L-IPSCs onto Mb terminals without AMPAR/KAR "priming" to remove the Mg^{2+} block (i.e., in the presence of an AMPAR/KAR antagonist) (Fig. 2*B*). This property of GABAergic feedback to Mbs is remarkably different from what has been reported in the mammalian retina, where NMDARs have not been found to contribute to either lateral or reciprocal GABAergic feedback (Chávez et al., 2006, 2010). Nonetheless, NMDARs have been shown to play a critical, direct role in releasing glycine from ACs in the mammalian retina (Chávez and Diamond, 2008).

Here, we have shown that GABAergic lateral feedback is mediated both by $GABA_A$Rs and $GABA_C$Rs. Nonetheless, we were unable to describe a temporal difference between the contributions of these two receptor classes to L-IPSCs that matched that of reciprocal feedback events (i.e., $GABA_A$Rs mediate fast and transient events, while $GABA_C$Rs activate more slowly and mediate sustained inhibition). Before this study, it was not known whether the same population of ACs could provide both lateral and reciprocal feedback inhibition to Mb terminals, depending on the spatial parameters of stimulation. However, when tested, we could not cross-deplete the GABAergic synaptic vesicle pools, or cross-desensitize the GABAergic synapses, that mediate reciprocal feedback by selectively activating lateral feedback inhibition with light stimulation (Fig. 5*Bii*), or vice versa (Fig. 5*C*). This suggests that different sets of GABAergic ACs are involved in reciprocal and lateral feedback inhibition in the goldfish retina, as has been previously suggested for rod BCs in rat retina (Chávez et al., 2010).

The vertebrate retina can be viewed as a spatiotemporal prefilter that channels different aspects of the visual scene to the brain for final processing (Meister and Berry, 1999; Field and Chililnisky, 2007; Joselevitch and Kamermans, 2009; Gollisch and Meister, 2010). Morphologically and physiologically diverse BCs play fundamental roles in this prefiltering process at the first retinal synapse, providing distinct postsynaptic processing of the photoreceptor signal (DeVries, 2000; DeVries et al., 2006). Here we have shown that three different populations of ACs filter the output of a given BC in the inner retina (i.e., ACs providing reciprocal, lateral ON, and lateral OFF feedback) under different light conditions. This exemplifies the idea that inhibitory interactions in the IPL are highly specialized for the task of shaping BC output to GCs (Roska and Werblin, 2001). Such complexity ensures that the temporal properties of BC output are highly regulated in a way that is likely critical for proper control of GC spike latencies, which are thought to be a key component of GC information coding in the retina (Gollisch and Meister, 2008).

References

Arai I, Tanaka M, Tachibana M (2010) Active roles of electrically coupled bipolar cell network in the adult retina. J Neurosci 30:9260–9270.

Awatramani GB, Slaughter MM (2001) Intensity-dependent, rapid activation of presynaptic metabotropic glutamate receptors at a central synapse. J Neurosci 21:741–749.

Bloomfield SA, Dacheux RF (2001) Rod vision: pathways and processing in the mammalian retina. Prog Retin Eye Res 20:351–384.

Bloomfield SA, Völgyi B (2007) Response properties of a unique subtype of wide-field amacrine cell in the rabbit retina. Vis Neurosci 24:459–469.

Brandstätter JH, Koulen P, Kuhn R, van der Putten H, Wässle H (1996) Compartmental localization of a metabotropic glutamate receptor (mGluR7): two different active sites at a retinal synapse. J Neurosci 16:4749–4756.

Busskamp V, Duebel J, Balya D, Fradot M, Viney TJ, Siegert S, Groner AC, Cabuy E, Forster V, Seeliger M, Biel M, Humphries P, Paques M, Mohand-Said S, Trono D, Deisseroth K, Sahel JA, Picaud S, Roska B (2010) Genetic reactivation of cone photoreceptors restores visual responses in retinitis pigmentosa. Science 329:413–417.

Chávez AE, Diamond JS (2008) Diverse mechanisms underlie glycinergic feedback transmission onto rod bipolar cells in rat retina. J Neurosci 28:7919–7928.

Chávez AE, Singer JH, Diamond JS (2006) Fast neurotransmitter release triggered by Ca influx through AMPA-type glutamate receptors. Nature 443:705–708.

Chávez AE, Grimes WN, Diamond JS (2010) Mechanisms underlying lateral GABAergic feedback onto rod bipolar cells in rat retina. J Neurosci 30:2330–2339.

Cook PB, McReynolds JS (1998) Lateral inhibition in the inner retina is important for spatial tuning of ganglion cells. Nat Neurosci 1:714–719.

Cousin MA, Nicholls DG (1997) Synaptic vesicle recycling in cultured cerebellar granule cells: role of vesicular acidification and refilling. J Neurochem 69:1927–1935.

Davenport CM, Detwiler PB, Dacey DM (2008) Effects of pH buffering on horizontal and ganglion cell light responses in primate retina: evidence for the proton hypothesis of surround formation. J Neurosci 28:456–464.

DeVries SH (2000) Bipolar cells use kainate and AMPA receptors to filter visual information into separate channels. Neuron 28:847–856.

DeVries SH, Baylor DA (1995) An alternative pathway for signal flow from rod photoreceptors to ganglion cells in mammalian retina. Proc Natl Acad Sci U S A 92:10658–10662.

DeVries SH, Li W, Saszik S (2006) Parallel processing in two transmitter microenvironments at the cone photoreceptor synapse. Neuron 50:735–748.

Dixon DB, Copenhagen DR (1992) Two types of glutamate receptors differentially excite amacrine cells in the tiger salamander retina. J Physiol 449:589–606.

Dong CJ, Werblin FS (1998) Temporal contrast enhancement via $GABA_C$ feedback at bipolar terminals in the tiger salamander retina. J Neurophysiol 79:2171–2180.

Dowling JE, Werblin FS (1969) Organization of retina of the mudpuppy, Necturus maculosus. I. Synaptic structure. J Neurophysiol 32:315–338.

Duebel J, Haverkamp S, Schleich W, Feng G, Augustine GJ, Kuner T, Euler T (2006) Two-photon imaging reveals somatodendritic chloride gradient in retinal ON-type bipolar cells expressing the biosensor Clomeleon. Neuron 49:81–94.

Eggers ED, Lukasiewicz PD (2006) $GABA_A$, $GABA_C$ and glycine receptor-mediated inhibition differentially affects light-evoked signalling from mouse retinal rod bipolar cells. J Physiol 572:215–225.

Eggers ED, Lukasiewicz PD (2010) Interneuron circuits tune inhibition in retinal bipolar cells. J Neurophysiol 103:25–37.

Euler T, Masland RH (2000) Light-evoked responses of bipolar cells in a mammalian retina. J Neurophysiol 83:1817–1829.

Fahrenfort I, Klooster J, Sjoerdsma T, Kamermans M (2005) The involvement of glutamate-gated channels in negative feedback from horizontal cells to cones. Prog Brain Res 147:219–229.

Fahrenfort I, Steijaert M, Sjoerdsma T, Vickers E, Ripps H, van Asselt J, Endeman D, Klooster J, Numan R, ten Eikelder H, von Gersdorff H, Kamermans M (2009) Hemichannel-mediated and pH-based feedback from horizontal cells to cones in the vertebrate retina. PLoS One 4:e6090.

Field GD, Chichilnisky EJ (2007) Information processing in the primate retina: circuitry and coding. Annu Rev Neurosci 30:1–30.

Flores-Herr N, Protti DA, Wässle H (2001) Synaptic currents generating the inhibitory surround of ganglion cells in the mammalian retina. J Neurosci 21:4852–4863.

Gauthier JL, Field GD, Sher A, Shlens J, Greschner M, Litke AM, Chichilnisky

EJ (2009) Uniform signal redundancy of parasol and midget ganglion cells in primate retina. J Neurosci 29:4675–4680.
Gillis KD (2000) Admittance-based measurement of membrane capacitance using the EPC-9 patch-clamp amplifier. Pflugers Arch 439:655–664.
Gollisch T, Meister M (2008) Rapid neural coding in the retina with relative spike latencies. Science 319:1108–1111.
Gollisch T, Meister M (2010) Eye smarter than scientists believed: neural computations in circuits of the retina. Neuron 65:150–164.
Grimes WN, Zhang J, Graydon CW, Kachar B, Diamond JS (2010) Retinal parallel processors: more than 100 independent microcircuits operate within a single interneuron. Neuron 65:873–885.
Hartveit E (1999) Reciprocal synaptic interactions between rod bipolar cells and amacrine cells in the rat retina. J Neurophysiol 81:2923–2936.
Hirasawa H, Kaneko A (2003) pH changes in the invaginating synaptic cleft mediate feedback from horizontal cells to cone photoreceptors by modulating Ca^{2+} channels. J Gen Physiol 122:657–671.
Hsueh HA, Molnar A, Werblin FS (2008) Amacrine-to-amacrine cell inhibition in the rabbit retina. J Neurophysiol 100:2077–2088.
Hull C, Studholme K, Yazulla S, von Gersdorff H (2006) Diurnal changes in exocytosis and the number of synaptic ribbons at active zones of an ON-type bipolar cell terminal. J Neurophysiol 96:2025–2033.
Ichinose T, Lukasiewicz PD (2005) Inner and outer retinal pathways both contribute to surround inhibition of salamander ganglion cells. J Physiol 565:517–535.
Jacobs AL, Werblin FS (1998) Spatiotemporal patterns at the retinal output. J Neurophysiol 80:447–451.
Joselevitch C, Kamermans M (2007) Interaction between rod and cone inputs in mixed-input bipolar cells in goldfish retina. J Neurosci Res 85:1579–1591.
Joselevitch C, Kamermans M (2009) Retinal parallel pathways: seeing with our inner fish. Vision Res 49:943–959.
Koulen P, Malitschek B, Kuhn R, Wässle H, Brandstätter JH (1996) Group II and group III metabotropic glutamate receptors in the rat retina: distributions and developmental expression patterns. Eur J Neurosci 8:2177–2187.
Krizaj D (2000) Mesopic state: cellular mechanisms involved in pre- and postsynaptic mixing of rod and cone signals. Microsc Res Tech 50:347–359.
Krizaj D, Akopian A, Witkovsky P (1994) The effects of L-glutamate, AMPA, quisqualate, and kainate on retinal horizontal cells depend on adaptational state: implications for rod-cone interactions. J Neurosci 14:5661–5671.
Li GL, Vigh J, von Gersdorff H (2007) Short-term depression at the reciprocal synapses between a retinal bipolar cell terminal and amacrine cells. J Neurosci 27:7377–7385.
Li P, Slaughter M (2007) Glycine receptor subunit composition alters the action of GABA antagonists. Vis Neurosci 24:513–521.
Lyubarsky AL, Falsini B, Pennesi ME, Valentini P, Pugh EN Jr (1999) UV- and midwave-sensitive cone-driven retinal responses of the mouse: a possible phenotype for coexpression of cone photopigments. J Neurosci 19:442–455.
Marc RE, Liu W (2000) Fundamental GABAergic amacrine cell circuitries in the retina: nested feedback, concatenated inhibition, and axosomatic synapses. J Comp Neurol 425:560–582.
Masland RH, Raviola E (2000) Confronting complexity: strategies for understanding the microcircuitry of the retina. Annu Rev Neurosci 23:249–284.
Matsui K, Hasegawa J, Tachibana M (2001) Modulation of excitatory synaptic transmission by $GABA_C$ receptor-mediated feedback in the mouse inner retina. J Neurophysiol 86:2285–2298.
McCall MA, Lukasiewicz PD, Gregg RG, Peachey NS (2002) Elimination of the rho1 subunit abolishes $GABA_C$ receptor expression and alters visual processing in the mouse retina. J Neurosci 22:4163–4174.
Meister M, Berry MJ 2nd (1999) The neural code of the retina. Neuron 22:435–450.
Menger N, Wässle H (2000) Morphological and physiological properties of the A17 amacrine cell of the rat retina. Vis Neurosci 17:769–780.
Molnar A, Werblin F (2007) Inhibitory feedback shapes bipolar cell responses in the rabbit retina. J Neurophysiol 98:3423–3435.
Molnar A, Hsueh HA, Roska B, Werblin FS (2009) Crossover inhibition in the retina: circuitry that compensates for nonlinear rectifying synaptic transmission. J Comput Neurosci 27:569–590.
Palacios AG, Varela FJ, Srivastava R, Goldsmith TH (1998) Spectral sensitivity of cones in the goldfish, Carassius auratus. Vision Res 38:2135–2146.
Palmer MJ (2010) Characterisation of bipolar cell synaptic transmission in goldfish retina using paired recordings. J Physiol 588:1489–1498.
Palmer MJ, Taschenberger H, Hull C, Tremere L, von Gersdorff H (2003) Synaptic activation of presynaptic glutamate transporter currents in nerve terminals. J Neurosci 23:4831–4841.
Pang JJ, Gao F, Wu SM (2007) Cross-talk between ON and OFF channels in the salamander retina: indirect bipolar cell inputs to ON-OFF ganglion cells. Vision Res 47:384–392.
Protti DA, Llano I (1998) Calcium currents and calcium signaling in rod bipolar cells of rat retinal slices. J Neurosci 18:3715–3724.
Protti DA, Gerschenfeld HM, Llano I (1997) GABAergic and glycinergic IPSCs in ganglion cells of rat retinal slices. J Neurosci 17:6075–6085.
Roska B, Werblin F (2001) Vertical interactions across ten parallel, stacked representations in the mammalian retina. Nature 410:583–587.
Saito T, Kondo H, Toyoda J (1981) Ionic mechanisms of two types of on-center bipolar cells in the carp retina. II. The responses to annular illumination. J Gen Physiol 78:569–589.
Shields CR, Lukasiewicz PD (2003) Spike-dependent GABA inputs to bipolar cell axon terminals contribute to lateral inhibition of retinal ganglion cells. J Neurophysiol 89:2449–2458.
Singer JH, Diamond JS (2006) Vesicle depletion and synaptic depression at a mammalian ribbon synapse. J Neurophysiol 95:3191–3198.
Slaughter MM, Miller RF (1981) 2-amino-4-phosphonobutyric acid: a new pharmacological tool for retina research. Science 211:182–185.
Sterling P (2004) How retinal circuits optimize the transfer of visual information. In: The visual neurosciences (Chalupa LM, Werner JS, eds), pp 234–259. Cambridge, MA: MIT.
Tatsukawa T, Hirasawa H, Kaneko A, Kaneda M (2005) GABA-mediated component in the feedback response of turtle retinal cones. Vis Neurosci 22:317–324.
Taylor WR (1999) TTX attenuates surround inhibition in rabbit retinal ganglion cells. Vis Neurosci 16:285–290.
Thoreson WB, Babai N, Bartoletti TM (2008) Feedback from horizontal cells to rod photoreceptors in vertebrate retina. J Neurosci 28:5691–5695.
Venkataramani S, Taylor WR (2010) Orientation selectivity in rabbit retinal ganglion cells is mediated by presynaptic inhibition. J Neurosci 30:15664–15676.
Vigh J, von Gersdorff H (2005) Prolonged reciprocal signaling via NMDA and GABA receptors at a retinal ribbon synapse. J Neurosci 25:11412–11423.
Vigh J, Witkovsky P (2004) Neurotransmitter actions on transient amacrine and ganglion cells of the turtle retina. Vis Neurosci 21:1–11.
Vigh J, Li GL, Hull C, von Gersdorff H (2005) Long-term plasticity mediated by mGluR1 at a retinal reciprocal synapse. Neuron 46:469–482.
von Gersdorff H, Matthews G (1999) Electrophysiology of synaptic vesicle cycling. Annu Rev Physiol 61:725–752.
Wässle H, Koulen P, Brandstätter JH, Fletcher EL, Becker CM (1998) Glycine and GABA receptors in the mammalian retina. Vision Res 38:1411–1430.
Watanabe S, Koizumi A, Matsunaga S, Stocker JW, Kaneko A (2000) GABA-mediated inhibition between amacrine cells in the goldfish retina. J Neurophysiol 84:1826–1834.
Witkovsky P, Dowling JE (1969) Synaptic relationships in the plexiform layers of carp retina. Z Zellforsch Mikrosk Anat 100:60–82.
Wong KY, Cohen ED, Dowling JE (2005) Retinal bipolar cell input mechanisms in giant danio. II. Patch-clamp analysis of ON bipolar cells. J Neurophysiol 93:94–107.
Zenisek D, Henry D, Studholme K, Yazulla S, Matthews G (2001) Voltage-dependent sodium channels are expressed in nonspiking retinal bipolar neurons. J Neurosci 21:4543–4550.
Zhang AJ, Wu SM (2009) Receptive fields of retinal bipolar cells are mediated by heterogeneous synaptic circuitry. J Neurosci 29:789–797.
Zhang J, Slaughter MM (1995) Preferential suppression of the ON pathway by GABAC receptors in the amphibian retina. J Neurophysiol 74:1583–1592.
Zhang J, Jung CS, Slaughter MM (1997) Serial inhibitory synapses in retina. Vis Neurosci 14:553–563.
Zhang J, Li W, Trexler EB, Massey SC (2002) Confocal analysis of reciprocal feedback at rod bipolar terminals in the rabbit retina. J Neurosci 22: 10871–10882.